Liposomes Labeled with Biotin and Horseradish Peroxidase: A Probe for the Enhanced Amplification of Antigen–Antibody or Oligonucleotide–DNA Sensing Processes by the Precipitation of an Insoluble Product on Electrodes

Lital Alfonta,[†] Anup K. Singh,[‡] and Itamar Willner*,[†]

The Institute of Chemistry, The Hebrew University of Jerusalem, Jerusalem 91904, Israel, and Chemical and Radiation Detection Laboratory, Sandia National Laboratories, Livermore, California 94550

Liposomes labeled with biotin and the enzyme horseradish peroxidase (HRP) are used as a probe to amplify the sensing of antigen–antibody interactions or oligonucleotide–DNA binding. The HRP-biocatalyzed oxidation of 4-chloro-1-naphthol (**1**) in the presence of H_2O_2, and the precipitation of the insoluble product **2** on electrode supports, are used as an amplification route for the sensing processes. The anti-dinitrophenyl antibody (DNP-Ab) is sensed by a dinitrophenyl-L-cysteine antigen monolayer associated with an Au electrode. A biotinylated anti-IgG-antibody (Fc-specific) is linked to the antigen–DNP-Ab complex, and the biotin-labeled HRP–liposomes associate with the assembly through an avidin bridge. The biocatalyzed precipitation of **2** on the electrode increases the electron-transfer resistances at the electrode–solution interface or the electrode resistance itself. The binding events of the different proteins on the electrode and the biocatalyzed precipitation of **2** on the conductive support are followed by Faradaic impedance spectroscopy or constant-current chronopotentiometry. DNP-Ab concentrations as low as 1×10^{-11} g·mL^{-1} can be detected by this method. The labeled liposomes were also used for the amplified detection of DNA **3**. The oligonucleotide **4**, complementary to a part of the target DNA **3** that is a model nucleic acid sequence for the Tay-Sachs genetic disorder, is assembled on an Au electrode. Hybridization of the analyte **3** followed by the association of the biotin-tagged oligonucleotide **5** yields a three-component double-stranded assembly. Sensing of the analyte **3** is amplified by the association of avidin, the labeled liposomes, and the subsequent biocatalyzed precipitation of **2** on the electrodes. The DNA **3** is detected with a sensitivity that corresponds to 6.5×10^{-13} M. Faradaic impedance spectroscopy and chronopotentiometry were employed to follow the stepwise assembly of the systems and the electronic transduction of the detection of the analyte DNA **3**.

The transduction of antigen–antibody or oligonucleotide–DNA recognition events is of substantial interest directed to the development of immunosensors and DNA sensor devices.[1,2] Electrochemical detection of antigen–antibody interactions has been the subject of many research efforts. The capacity changes at the electrode–electrolyte interface as a result of the formation of antigen–antibody complexes on the electrode were applied to develop a series of capacitive affinity sensors.[3] Amperometric detection of antigen–antibody interactions was accomplished by the application of redox-modified antigens or antibodies and their competitive association to the electrode support in the presence of the analyte antigen or antibody, respectively.[4,5] Microgravimetric, quartz crystal-microbalance, transduction of antigen–antibody binding phenomena were reported as alternative electronic transduction means for immunosensor devices.[6,7] Electrochemical

* To whom correspondence should be addressed: (tel) 972-2-6585272; (fax) 972-2-6527715; (e-mail) willnea@vms.huji.ac.il.
† The Hebrew University of Jerusalem.
‡ Sandia National Laboratories.
(1) (a) Willner, I.; Katz, E.; Willner, B. In *Sensors Update*; Baltes, H., Göpel, W., Hesse, J., Eds.; Wiley-VCH: Weinheim, 1999; Vol. 5; pp 45–102. (b) Willner, I.; Katz, E. *Angew. Chem., Int. Ed.* **2000**, *39*, 1181–1218. (c) Gebauer, C. R. In *Electrochemical Sensors in Immunological Analysis*; Ngo, T. T., Ed.; Plenum Press: New York, 1987; pp 239–255. (d) Suleiman, A. A.; Guilbault, G. G. *Anal. Lett.* **1991**, *24*, 1283–1292. (e) Anderson, J. L.; Bowden, E. F.; Pickup, P. G. *Anal. Chem.* **1996**, *68*, 379R-444R. (f) Göpel, W.; Heiduschka, P. *Biosens. Bioelectron.* **1995**, *10*, 853–883. (g) Aizawa, M. In *Biosensor Principles and Applications*; Blum, L. J., Coulet, P. R., Eds.; Marcel Dekker: New York, 1991; pp 249–266.
(2) (a) Wilson, E. K. *Chem. Eng. News* **1998**, *76* (21), 47–49. (b) Mikkelsen, S. R. *Electroanalysis* **1996**, *8*, 15–19. (c) Yang, M. S.; McGovern, M. E.; Thompson, M. *Anal. Chim. Acta* **1997**, *346*, 259–275. (d) Thompson, M.; Furtado, M. *Analyst* **1999**, *184*, 1133–1136.
(3) Bresler, H. S.; Lenkevich, M. J.; Murdock, J. F.; Newman, A. L.; Roblin, R. O. In *Biosensor Design and Application*; Mathewson, P. R., Finley, J. W., Eds.; ACS Symposium Series 511; American Chemical Society: Washington, DC, 1992; pp 89–104.
(4) (a) Weber, S. G.; Purdy, W. C. *Anal. Lett.* **1979**, *12*, 1–9. (b) Doyl, J. M.; Wehmeyer, K. R.; Heineman, W. R.; Halsall, H. B. In *Electrochemical Sensors in Immunological Analysis*; Ngo, T. T., Ed.; Plenum Press: New York, 1987; pp 87–102.
(5) (a) Di Gleria, K.; Hill, H. A. O.; McNeil, C. J.; Green, M. J. *Anal. Chem.* **1986**, *58*, 1203–1205. (b) Di Gleria, K.; Hill, H. A. O.; Chambers, J. A. *J. Electroanal. Chem.* **1989**, *267*, 83–91. (c) Chambers, J. A.; Walton, N. J. *J. Electroanal. Chem.* **1988**, *250*, 417–425.
(6) (a) Suleiman, A. A.; Guilbault, G. G. *Analyst* **1994**, *119*, 2279–2282. (b) Kösslinger, C.; Drost, S.; Aberl, F.; Wolf, H.; Koch, S.; Woias, P. *Biosens. Bioelectron.* **1992**, *7*, 397–404.
(7) (a) Guilbault, G. G.; Hock, B.; Schmid, R. *Biosens. Bioelectron.* **1992**, *7*, 411–419. (b) König, B.; Grätzel, M. *Anal. Chem.* **1994**, *66*, 341–344.

transduction of oligonucleotide−DNA binding events was accomplished by the use of oligonucleotide-functionalized conductive polymers,[8] the application of electroactive dyes,[9] transition-metal complexes,[10] or redox-active intercalators[11] that bind to the resulting double-stranded oligonucleotide−DNA assembly.

The amplified electronic transduction of antigen/antibody or DNA sensing processes is a major challenge in the development of these bioelectronic devices. Amplified detection of antigen−antibody interactions was accomplished by the coupling of enzymes to the antigen or antibody probes that participate in the sensing events.[12,13] The biocatalyzed generation of electroactive species or the participation of O_2, H_2O_2 or NH_3 in the enzyme-stimulated processes enabled the amplified amperometric or voltammetric transduction of the antigen−antibody binding events.[14] Electrically wired enzymes were used as amplifying redox labels for antigen−antibody interactions on electrode supports.[15] The insulation of the conducting support by the antigen−antibody complex perturbs the electrical contact between the enzyme and the electrode and enables the amplified amperometric transduction of the antigen−antibody interactions through the bioelectrocatalyzed transformation. Indirect amplified detection of antigen−antibody interactions was reported by the application of enzymes that biocatalyze the formation of a polymer or an insoluble product on the electrode or the piezoelectric crystal, as a result of the antigen−antibody recognition process.[16,17] Microgravimetric quartz crystal microbalance analysis,[16,17] Faradaic impedance spectroscopy[17] or chronopotentiometry[18] was used as electronic transduction method of the amplified sensing signals.

The amplified detection of DNA was reported by the application of oligonucleotide-functionalized redox enzymes[19] that act as bioelectrocatalytic probes for the formation of the double-stranded DNA complex or the use of dendritic oligonucleotides as a branched sensing interface for the analyte DNA.[20] Specific anti-double-stranded DNA antibodies[21] or proteins[22] were used to bind as specific biomolecular amplifying probes to the oligonucleotide−DNA assemblies on the electronic transducers. The selective association of enzymes to the double-stranded oligonucleotide−DNA assembly, and the subsequent biocatalyzed precipitation of an insoluble product on the transducers, were used as an amplification path for the oligonucleotide−DNA recognition event.[23] Charged oligonucleotide-functionalized liposomes or biotin-labeled liposomes were used for the dendritic amplification of oligonucleotide−DNA binding events.[24,25] The control of the surface properties of electronic transducers by the liposome micromembranes provides a means to amplify the DNA sensing events. In all of these systems, Faradaic impedance spectroscopy and microgravimetric quartz crystal microbalance measurements served as electronic transduction methods for the amplified sensing pathways. Recently, oligonucleotide-functionalized Au nanoparticles were used for the dendritic amplification of DNA sensing through the microgravimetric transduction of the oligonucleotide−DNA complex formation using an Au/quartz crystal as transducer.[26] Here we report on the application of biotin-labeled horseradish peroxidase (HRP)-functionalized liposomes as a novel probe for the two-step amplification of antigen−antibody and DNA sensing processes. Liposomes, owing to their large surface area and a large internal volume, are capable of carrying a large number of marker and receptor molecules. This has led to widespread employment as drug delivery vehicles as well as signal enhancement agents in immunoassays and biosensor applications.[27] We apply Faradaic impedance spectroscopy or chronopotentiometry to characterize the biorecognition events and the amplification routes upon sensing the respective antibody or DNA.

EXPERIMENTAL SECTION

Chemicals. Horseradish peroxidase, type VI-A, 2,2′-azinobis-3-ethylbenzothiazoline-6-sulfonic acid (ABTS), hydrogen peroxide, dimyristoylphosphatidylethanolamine (DMPE), distearoylphosphatidylcholine (DSPC), cholesterol, sodium m-periodate, phosphate-buffered saline (PBS), N,N-bis(2,4-dinitrophenyl)-L-cysteine, goat IgG-anti-DNP, avidin, 4-chloro-1-naphthol, and all other chemicals were from a commercial source (Aldrich or Sigma) and were used as supplied without further purification.

Ethylene glycol was obtained from Fisher Scientific, Biotin-X-DMPE was obtained from Molecular Probes (Eugene, OR). Monoclonal rabbit IgG-anti-goat-IgG Fc specific conjugate with biotin was from Biotest. Oligonucleotides were custom-made (General Biotechnology, Rehovot, Israel).

(8) Korri-Youssoufi, H.; Garnier, F.; Srivstava, P.; Godillot, P.; Yassar, A. *J. Am. Chem. Soc.* **1997**, *119*, 7388−7389.

(9) Hashimoto, K.; Ito, K.; Ishimori, Y. *Anal. Chem.* **1994**, *66*, 3830−3833.

(10) Millan, K. M.; Saraullo, A.; Mikkelsen, S. R. *Anal. Chem.* **1994**, *66*, 2943−2948.

(11) Takenaka, S.; Yamashita, K.; Takagi, M.; Oto, Y.; Kondo, H. *Anal. Chem.* **2000**, *72*, 1334−1341.

(12) (a) Ho, W. O.; Athey, D.; McNeil, C. J. *Biosens. Bioelectron.* **1995**, *10*, 683−691. (b) Rishpon, J.; Soussan, L.; Rosen-Margalit, I.; Hadas, E. *Immunoassays* **1992**, *13*, 231−235.

(13) (a) Wright, D. S.; Halsall, H. G.; Heineman, W. R. In *Electrochemical Sensors in Immunological Analysis*; Ngo, T. T., Ed.; Plenum Press: New York, 1987; pp 117−130. (b) Tang, H. T.; Halsall, H. B.; Heineman, W. R. *Clin. Chem.* **1991**, *37*, 245−248. (c) Wehmeyer, K. R.; Halsall, H. B.; Heineman, W. R.; Volle, C. P.; Chen, C. *Anal. Chem.* **1986**, *58*, 135−139.

(14) (a) Aizawa, M. In *Electrochemical Sensors in Immunological Analysis*; Ngo, T. T., Ed.; Plenum Press: New York, 1987; pp 269−291. (b) Franconi, C.; Bonori, M.; Orsega, E. F.; Scarpa, M.; Rigo, A. *J. Pharm. Biomed. Anal.* **1987**, *5*, 283−287. (c) Uditha de Alwis, W.; Wilson, G. S. *Anal. Chem.* **1985**, *57*, 2754−2756. (d) Tsuji, I.; Eguchi, H.; Yasukouchi, K.; Unoki, M.; Taniguchi, I. *Biosens. Bioelectron.* **1990**, *5*, 87−101.

(15) (a) Blonder, R.; Katz, E.; Cohen, Y.; Norbert, I.; Riklin, A.; Willner, I. *Anal. Chem.* **1996**, *68*, 3151−3157. (b) Blonder, R.; Levi, S.; Tao, G.; Ben-Dov, I.; Willner, I. *J. Am. Chem. Soc.* **1997**, *119*, 10467−10478.

(16) Ebersole, R. C.; Ward, M. D. *J. Am. Chem. Soc.* **1988**, *110*, 8623−8628.

(17) Bardea, A.; Katz, E.; Willner, I. *Electroanalysis* **2000**, *12*, 1097−1106.

(18) Alfonta, L.; Bardea, A.; Khersonsky, O.; Katz, E.; Willner, I. *Biosens. Bioelectron.*, in press.

(19) de Lumley Woodyear, T.; Campbell, C. N.; Heller, A. *J. Am. Chem. Soc.* **1996**, *118*, 5504−5505.

(20) Wang, J.; Jiang, M.; Nilsen, T. W.; Getts, R. C. *J. Am. Chem. Soc.* **1998**, *120*, 8281−8282.

(21) Bardea, A.; Dagan, A.; Ben-Dov, I.; Amit, B.; Willner, I. *Chem. Commun.* **1998**, 839−840.

(22) Bardea, A.; Patolsky, F.; Dagan, A.; Willner, I. *Chem. Commun.* **1999**, 21−22.

(23) Patolsky, F.; Katz, E.; Bardea, A.; Willner, I. *Langmuir* **1999**, *15*, 3703−3706.

(24) Patolsky, F.; Lichtenstein, A.; Willner, I. *Angew. Chem., Int. Ed.* **2000**, *39*, 940−943.

(25) Patolsky, F.; Lichtenstein, A.; Willner, I. *J. Am. Chem. Soc.* **2000**, *122*, 418−419.

(26) Patolsky, F.; Ranjit, K. T.; Willner, I. *Chem. Commun.* **2000**, 1025−1026.

(27) (a) Singh, A. K.; Kilpatrick, P. K.; Carbonell, R. G. *Biotechnol. Prog.* **1996**, *12*, 272−280. (b) Singh, A. K.; Carbonell, R. G. In *Nonmedical Applications of Liposomes*; Lasic, D. L., Barenholz, Y., Eds.; CRC Press: Boca Raton, FL, 1995; pp 209−228. (c) Singh, A. K.; Schoeniger, J. S.; Carbonell, R. G. In *Biosensors and Their Applications*; Yang, V. C., Ngo, T. T., Eds.; Kluwer Academic/Plenum Publishing: New York, 2000; pp 131−145.

Ultrapure water from Elgastat (UHQ) source was used throughout this work.

Electrode Characterization and Pretreatment. Gold wire electrodes (0.5-mm diameter, ~0.2-cm² geometrical area, roughness coefficient, ~1.2−1.5) were used for the electrochemical measurements. To remove any previous organic layer, and to regenerate a bare metal surface, the electrodes were treated in a boiling 2 M solution of KOH for 4 h, then rinsed with water, and stored in concentrated sulfuric acid. Immediately before modification, the electrodes were rinsed with water, soaked for 10 min in concentrated nitric acid, and then rinsed with water again.

Electrochemical Measurements. A conventional three-electrode cell, consisting of the modified Au electrode, a glassy carbon auxiliary electrode isolated by a glass frit, and a saturated calomel electrode (SCE) connected to the working volume with a Luggin capillary, was used for the electrochemical measurements. The cell was positioned in a grounded Faradaic cage. Impedance and chronopotentiometry measurements were performed using an electrochemical impedance analyzer (EG&G, model 1025) and potentiostat (EG&G, model 283) connected to a computer (EG&G Software Power Suite 1.03 and 270/250 for impedance and chronopotentiometry, respectively). All electrochemical measurements were performed in 0.1 M phosphate buffer, pH 7.0, as a background electrolyte solution.

Chronopotentiometry and Faradaic impedance measurements were performed in the presence of a 10 mM $K_3[Fe(CN)_6]/K_4[Fe(CN)_6]$ (1:1) mixture, as a redox probe (using an alternating voltage, 10 mV). Impedance measurements were performed at a bias potential of 0.17 V vs SCE in the frequency range from 100 mHz to 50 kHz. The impedance spectra were plotted in the form of complex plane diagrams (Nyquist plots). Chronopotentiometry measurements were performed at a set current of 10 μA and a pulse duration of 10 s. The potential developed at the end of the pulse (after 10 s) was used to derive the electrode resistance.

Electrode Modifications. *DNA-Sensing Interface.* The methods to analyze the target DNA−analyte and to assemble the DNA sensor bioelectronic system are depicted in Scheme 2. The 18-mer oligonucleotide **4**, includes a 12-base sequence that is complementary to a part of the analyte, the Tay-Sachs (TS) mutant **3**. In addition, it includes a 5-base thiophosphate thymine-Ts tag for its assembly on the Au electrode and a single T-base separating the tag from the sensing oligonucleotide sequence. The clean Au electrode was interacted with **4** (50 μg·mL⁻¹, 10 h, 4 °C), resulting in the assembly of the sensing interface on the gold support. The resulting **4**-functionalized electrode was interacted with a solution that includes the target analyte, the TS mutant **3** (varying concentrations, 1 h, room temperature). The resulting double-stranded assembly of **4** and **3**-functionalized electrode was reacted with the biotinylated oligonucleotide **5** (500 ng·mL⁻¹, 1 h, room temperature). The biotin-labeled oligonucleotide is complementary to the analyte part of the double-stranded assembly associated with the electrode. The resulting bifunctional, biotin-tagged, three-component double-stranded DNA−oligonucleotide assembly was subsequently treated with avidin (200 ng·mL⁻¹, 20 min, room temperature). The final configuration was reacted with the biotinylated HRP-modified liposome (1.46 × 10⁻¹¹ M, 30 min, room temperature).

Immunosensor Modification Assay. The modification of the Au electrode surface with dinitrophenyl antigen was performed by the incubation of the clean electrode in a 2 mM aqueous solution of *N,N*-bis(2,4-dinitrophenyl)-L-cysteine for 2 h, followed by rinsing of the electrode with water. The dinitrophenyl (DNP)-antigen-functionalized electrode was reacted with complementary analyte−antibody, goat IgG-anti-DNP, and DNP-Ab (variable concentrations) in 0.1 M phosphate buffer, pH 7.3, for 5 min and then rinsed with phosphate buffer to yield the antigen−antibody complex on the electrode. The resulting electrode was reacted with 15 μg·mL rabbit IgG-anti-goat−Fc-specific-biotin conjugate in phosphate buffer for 5 min and then rinsed with phosphate buffer to yield the antigen−antibody−anti-antibody−biotin complex on the electrode. The resulting modified electrode was further reacted with avidin (100 ng·mL⁻¹, 15 min in PBS , at room temperature). The resulting assembly on the electrode was further reacted with the biotin-tagged HRP-functionalized liposomes (1.46 × 10⁻¹¹ M for 30 min in saline phosphate buffer, at room temperature).

Analytical Procedure. 4-Chloro-1-naphthol (**1**) was dissolved initially in ethanol and then the ethanolic stock solution was diluted with 0.1 M phosphate buffer, pH 7.3, to yield the developing solution that includes l × 10⁻³ M of **1** and 2% (v/v) ethanol. The modified electrodes consisting of the HRP-tagged liposomes and oligonucleotide−DNA-functionalized electrodes or the antigen−antibody−anti-antibody−avidin−biotinylated-HRP-tagged liposome-functionalized-electrodes were incubated for a specified and controlled time interval in a probe solution consisting of **1**, 1 × 10⁻³ M, and H_2O_2, 1.5 × 10⁻⁴ M. After incubation of the respective electrodes in the probe solution, the electrodes were rinsed with 0.1 M phosphate buffer, pH 7.3, and introduced into the electrochemical cell for the respective analyses (Faradaic impedance spectroscopy or chronopotentiometry).

Liposome Preparation. Unilamellar liposomes containing DSPC/cholesterol/DMPE/DHPE-X-biotin in molar ratio of 40:40:19.5:0.5 were prepared by extrusion through polycarbonate membranes as described by Hope et al.[28] Extrusion was carried out using a pneumatic automatic liposome extruder (Liposofast, Avestin, Inc., Vancouver, Canada). The resulting unilamellar liposomes were centrifuged at 3000 rpm for 20 min to remove residual multilamellar vesicles and aggregated lipids. The liposome solution was stored at 4 °C until further use.

HRP was covalently linked to liposomes using the periodate oxidation method described previously.[29] HRP, 5 mg·mL⁻¹, in 50 mM citrate buffer (CB), pH 6.0, was oxidized with 10 mM sodium periodate for 30 min at 25 °C in the dark with gentle stirring. Excess periodate was neutralized by the addition of 0.5 mL of 0.6 M ethylene glycol for 1 h at 25 °C. Unreacted reagents were removed by desalting on a 10-cm Econo-Pac 10DG desalting column (Bio-Rad Laboratories, Richmond, CA) equilibrated with 25 mM borate, pH 8.5. The activated HRP was added to 1 mL of 3 mg of lipid·mL⁻¹ liposomes. The reaction was carried out at 25 °C with gentle stirring. To reduce the Schiff base formed between HRP and DMPE, 250 μL of 20 mg·mL⁻¹ $NaCNBH_3$ was added and the solution was incubated for 16−18 h at 4 °C. The reaction mixture was applied to a 70 × 1.5 cm size exclusion column

(28) Mayer, L. D.; Hope, M. J.; Cullis, P. R. *Biochim. Biophys. Acta* **1986**, *858*, 161−168.
(29) Singh, A. K.; Kilpatrick, P. K.; Carbonell, R. G. *Biotechnol. Prog.* **1995**, *11*, 333−341.

Table I. Properties of HRP-Functionalized Liposomes

	HRP−biotin liposomes	HRP liposomes (control)
composition	DSPC/cholesterol/DMPE/ DHPE-X-biotin (40:40:19.5:0.5 mol %)	DSPC/cholesterol/DMPE (40:40:20 mol %)
concentration	1.46 nM	1.48 nM
hydrodynamic diameter	148 nm	142 nm
ζ potential (at pH 7 in 1 mM KCl)	−33.7 mV	−35.9 mV
HRP/liposome	178	198
biotin/liposome	1214	0
specific enzyme activity	8.55×10^{-4} Abs·mL/min·mg	8.38×10^{-4} Abs·mL/min·mg

packed with Sephacryl S-300-HR and equilibrated with 0.05 M Borax/borate buffer at pH 8.5. The flow rate was maintained at 0.125 mL·min^{-1} using a peristaltic pump (MP-1, Spectrum) and 0.5-mL fractions were collected using an automatic fraction collector. The fractions were analyzed by assaying for HRP activity as discussed later.

Characterization of Liposomes. Hydrodynamic diameters of unilamellar liposomes were estimated by dynamic light scattering (DLS) using a commercial device (Zet Plus, Brookhaven Instruments Corp.). Samples for size measurement were prepared by addition of 25 μL of liposomes to 2 mL of 10 mM phosphate buffer, pH 7.2. The solution was filtered using a 0.2-μm syringe filter and dispensed into a clean plastic cuvette. Measurements were performed at a 90° scattering angle using a 633-nm diode laser, and correlation function was generated by a BI-9000AT digital correlator. The data were analyzed using the constrained regularization method,[30] resulting in a size distribution characterized by a mean diameter and variance.

Kinetic parameters for HRP immobilized on the surface of the liposomes were determined using Michaelis−Menten kinetics, given by

$$V = V_{max}S/(K_m + S)$$

where V is the reaction rate, S is the substrate concentration, V_{max} is the maximum reaction rate, and K_m is the Michaelis constant. The kinetics parameters K_m and V_{max} were determined from a plot of reaction rate versus substrate concentration using a nonlinear least-squares fit of the experimental data. The maximal reaction rate, V_{max}, can also be written as $V_{max} = k_p E_0$, where k_p is the enzyme specific activity (also called k_{cat}) and E_0 is the enzyme concentration. Activity measurements were performed in 50 mM citrate buffer, pH 4.0 using 2,2′-azinobis-3-ethylbenzothiazoline-6-sulfonic acid (ABTS) and H_2O_2 as substrates at 25 °C. A 3.2-mL aliquot of substrate (2 mM ABTS and 2.75 mM H_2O_2) was pipetted into sample and reference cuvettes. Ten microliters of enzyme solution was added to the sample and blanked against buffer, and the change in absorbance was recorded at 410 nm with a UV−visible spectrophotometer. The immobilized HRP concentration was determined by measuring the absorbance of the liposome solution at 403 nm, subtracting the contribution due to scattering by liposomes from the total absorbance, and using an extinction coefficient of 74 000 M^{-1} cm^{-1}.

The concentration of phospholipids in a liposome sample and ultimately the liposome concentration were determined by a phosphate assay using the method of Chen et al.[31] Knowing the diameter of a liposome and the projected headgroup areas of constituent lipids, the total number of lipids in a liposome, and hence the liposome concentration, the number of HRP per liposome and the number of biotin units per liposome can be determined.

RESULTS AND DISCUSSION

Application of Enzyme-Labeled Liposomes for the Electronic Transduction of Antigen−Antibody and Nucleic Acid−DNA Interactions. The probe that was used in the present study as an amplifier for antigen/antibody or DNA sensing events consists of biotin-labeled-HRP-functionalized liposomes. Table 1 summarizes the properties of HRP-functionalized liposomes. The liposome surfaces are highly negatively charged, thereby preventing nonspecific adsorption of the liposomes to proteins or DNA associated with the sensing interface. The biotin tag provides an anchoring site that links the biocatalytic liposome probe to the biorecognition assembly. The enzyme HRP incorporated in the liposome will stimulate the H_2O_2-biocatalyzed oxidation of **1** to the insoluble product **2** (Scheme 1). Scheme 1 outlines the concept for the amplified electronic transduction of the sensing of an antibody. An antigen is assembled on the electrode and acts as the sensing interface. In the presence of the analyte antibody, the antigen−antibody complex is formed at the electrode interface. Interaction of the resulting interface with the anti-antibody−biotin conjugate results in the "sandwich complex" on the sensing interface. Interaction of the resulting assembly with avidin and then biotin-labeled HRP liposome probe leads to the association of the biocatalytic probe to the interface. The probe biocatalyzes the precipitation of the insoluble product **2** on the electrode. Note that the antigen−antibody recognition event leads to the association of a "giant" negatively charged micromembrane on the electrode, and thus, the electrical as well as capacity features of the interface will be significantly altered. Furthermore, the biocatalytic precipitation of **2** on the electrode results in the insulation of the electrode support and provides an amplification path for the primary antigen−antibody complex on the conductive support. Scheme 2 exemplifies the method to analyze a target DNA **3**. An oligonucleotide **4**, complementary to a part of the target DNA, is assembled on the electrode and acts as the sensing interface. In the presence of the target DNA, the double-stranded (ds) assembly is formed on the electrode. Further interactions of the ds assembly with a biotin-labeled oligonucleotide **5**, which is complementary to the other end of the target DNA, results in the

(30) Provencher, S. W. *Comput. Phys. Comm.* **1982**, *27*, 213−227.

(31) Chen, P. S.; Toribara, T. Y.; Warner, H. *Anal. Chem.* **1956**, *28*, 1756−1758.

Scheme 1. Amplified Sensing of the Anti-DNP Antibody by a Biotin-Tagged HRP-Functionalized Liposome and the Electronic Transduction of the Sensing Event by Following the Interfacial Electron-Transfer Resistance as a Result of the Biocatalyzed Precipitation of 2
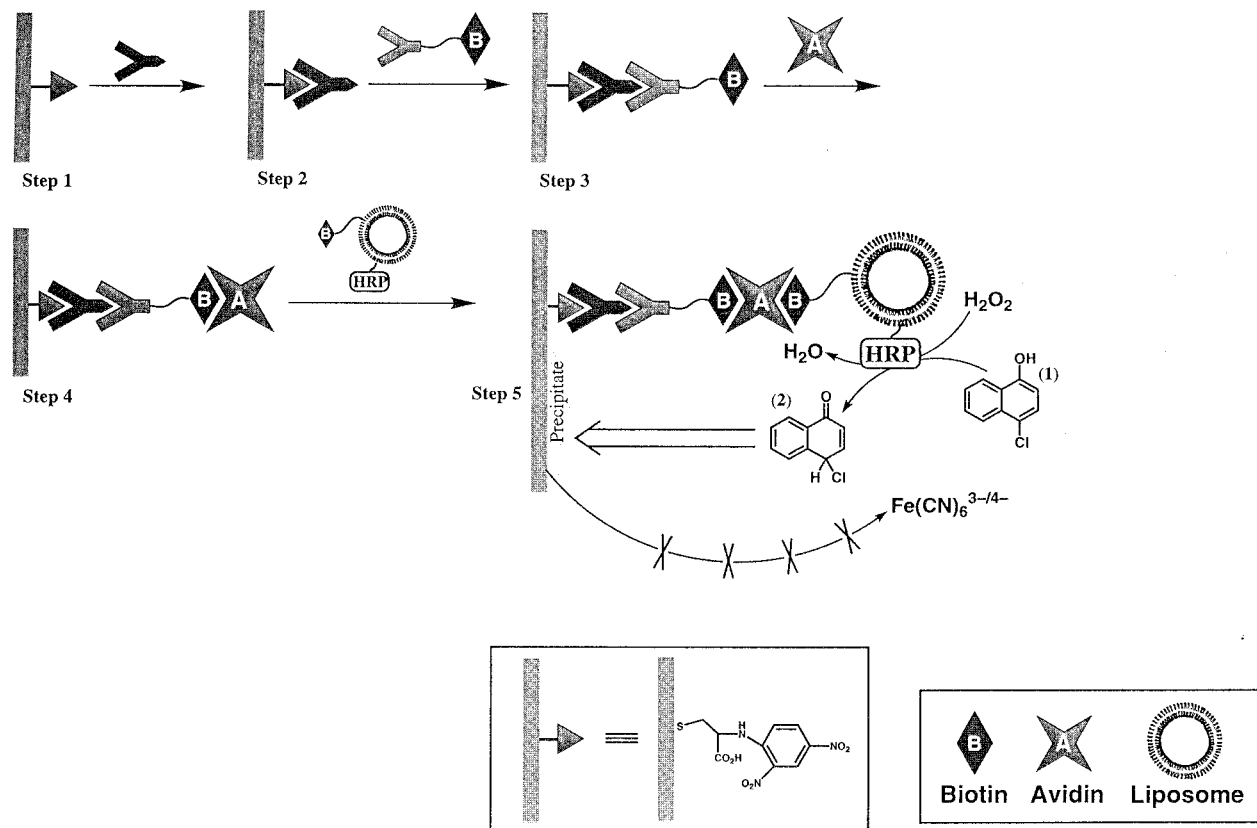
tricomponent ds complex on the surface. The resulting interface is then reacted with avidin and subsequently with the biotin-labeled HRP-functionalized liposome probe. Note that binding of the liposome probe and the secondary biocatalyzed precipitation of the insoluble product on the surface occurs only if the primary target DNA binds to the sensing interface. Thus, the biotin-labeled HRP liposomes provide a dual-amplification route for the sensing events, the giant liposome micromembrane alters the interfacial properties of the electrode as a result of the biorecognition event, and the biocatalyzed precipitation of **2** on the electrode represents the accumulation of an insulating layer on the electrode as a result of the recognition processes. Note that the amount of liposomes associated with the electrode is controlled by the respective analyte−antibody or target DNA. The amount of precipitate **2** that is accumulated on the conductive support is controlled by the content of the biocatalytic probe associated with the sensing interface, as well as by the time interval employed for the biocatalyzed precipitation process. This implies that the formulated methods may be employed for the quantitative analyses of the antibody or DNA. Also, the sensitivity of the respective sensing routes may be tuned by the time interval used for the precipitation of the insoluble product **2**.

The alteration of the interfacial properties of the electrode support by the association of the liposomes or upon the precipitation of the insoluble product may be followed by Faradaic impedance spectroscopy[32] and chronopotentiometry.[33]

Impedance spectroscopy is an effective method for probing the features of surface-modified electrodes. The complex imped-

ance can be presented as the sum of the real, $Z_{re}(\omega)$, and imaginary, $Z_{im}(\omega)$ components that originate mainly from the resistance and capacitance of the cell, respectively.
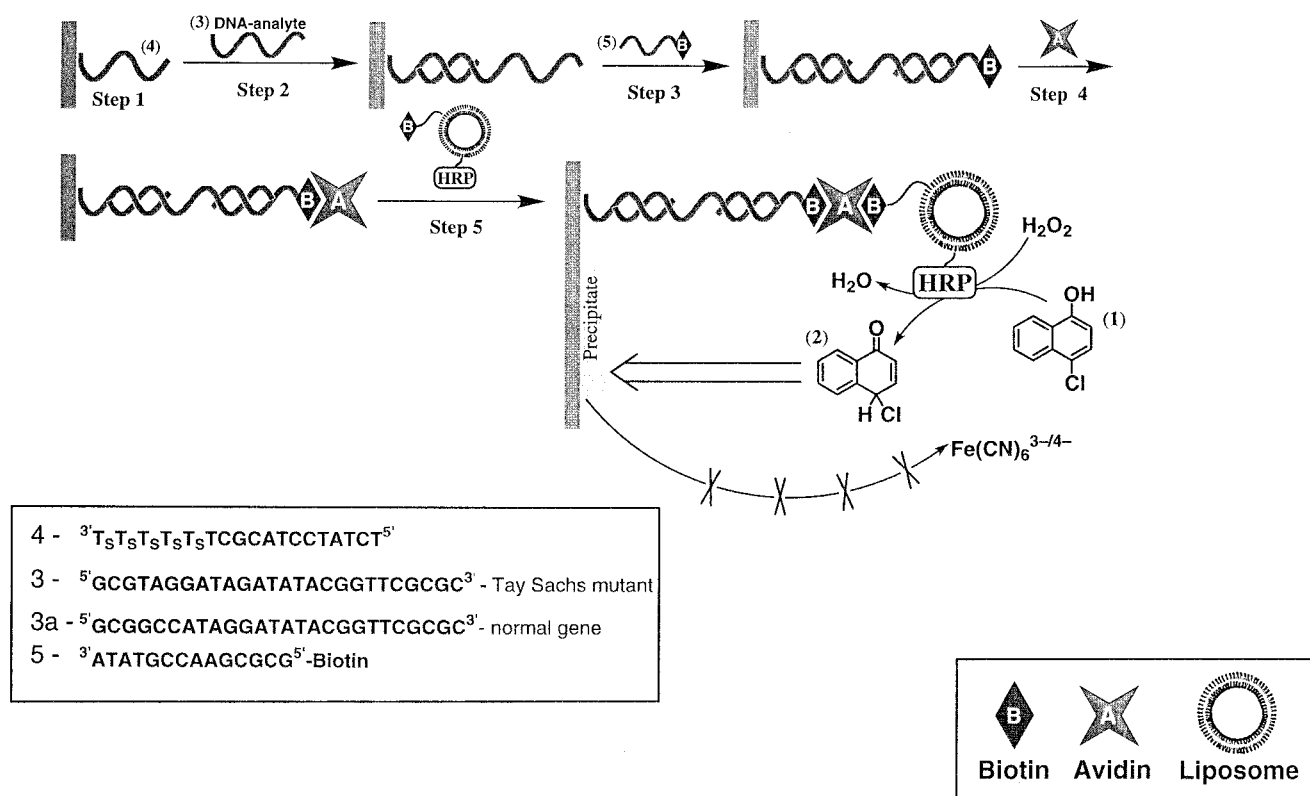
The modification of the metallic surface with a biomaterial or an organic layer decreases the double-layer capacitance and retards the interfacial electron-transfer rates. The electron-transfer resistance at the electrode will be given by eq 1, where

$$R_{et} = R_{Au} + R_{mod} \qquad (1)$$

R_{Au} and R_{mod} are the electron-transfer resistance of the nonmodified electrode and the variable electron-transfer resistance introduced by the modifier, in the presence of the solubilized redox probe, respectively. A typical shape of a Faradaic impedance spectrum (presented in the form of a Nyquist plot, Z_{im} vs Z_{re}), includes a semicircle region lying on the Z_{re} axis followed by a straight line. The semicircle portion, observed at higher frequencies, corresponds to the electron-transfer-limited process, whereas the linear part is characteristic of the lower frequencies range and represents the diffusional-limited electron-transfer process.

(32) (a) Bard, A. J.; Faulkner, L. R. *Electrochemical Methods: Fundamentals and Applications*; Wiley: New York, 1980. (b) Bond, A. M. *Modern Polarographic Methods in Analytical Chemistry*; Marcel Dekker: New York, 1980. (c) Macdonald, J. R. *Impedance Spectroscopy Emphasizing Solid Materials and Systems*; Wiley: New York, 1987.

(33) (a) Wang, J.; Cai, X. H.; Rivas, G.; Shiraishi, H.; Dontha, N. *Biosens. Bioelectron.* **1997**, *12*, 587−599. (b) Cai, X. H.; Rivas, G.; Farias, P. A. M.; Shiraishi, H.; Wang, J.; Palecek, E. *Anal. Chim. Acta* **1996**, *332*, 49−57.

Scheme 2. Amplified Detection of a Target DNA by Biotin-Tagged-HRP-Functionalized Liposomes and the Biocatalyzed Precipitation of an Insoluble Product on the Electrode

4 - $^{3'}T_sT_sT_sT_sT_sTCGCATCCTATCT^{5'}$

3 - $^{5'}GCGTAGGATAGATATACGGTTCGCGC^{3'}$ - Tay Sachs mutant

3a - $^{5'}GCGGCCATAGGATATACGGTTCGCGC^{3'}$ - normal gene

5 - $^{3'}ATATGCCAAGCGCG^{5'}$-Biotin

Biotin   Avidin   Liposome

Faradaic impedance spectroscopy is an efficient method to probe and model the interfacial properties of electrodes, yet it suffers from the long time interval required to record a full spectrum in a broad frequency range. This limitation may be partially resolved by the application of constant-current chronopotentiometry.

Chronopotentiometry is an electrochemical technique that applies a constant and controlled current between the working and auxiliary electrodes, while the potential between the working electrode and the reference electrode is altered to retain the desired current value. In the presence of a reversible redox probe in the solution, a Nernstian electrochemical process occurs upon the application of the constant-current value, and the electrode potential is shifted to the characteristic potential of the redox probe in solution. The potential of the electrode is constantly altered according to the R_{ox}/R_{red} ratio of the redox label at the electrode surface. Provided a cathodic current is driven through the solution, after a transition time, τ, the concentration of the oxidized redox species, R_{ox}, at the electrode, drops to zero. Under these conditions, and in the absence of any other redox probe in solution, the potential on the electrode will be sharply shifted to negative values, corresponding to the cathodic discharge of the electrolyte (or the reduction of oxygen), to retain the passage of the desired current value. The association of the liposomes to the electrode surface, and the subsequent biocatalyzed precipitation of an insulating layer on the electrode support, are anticipated to inhibit the interfacial electron-transfer rate. Thus, to retain the set current value in the cell, the application of an overpotential, η, on the electrode is required. The overpotential on the electrode will relate to the change in the electrode resistance, R', as a result of modification (formation of the insoluble precipitate) as given by

eq 2, where I is the set constant current and R'_{mod} and R'_{Au}

$$R' = \eta/I = R'_{mod} - R'_{Au} \qquad (2)$$

correspond to the resistances of the modified electrode and the bare electrode, respectively. The slope of the $E-t$ curve in the presence of a modifier (or a precipitate) on the electrode is different from the respective curve corresponding to reversible Nernstian behavior of the redox probe since the electron-transfer rate is lower in the presence of the modifier. Thus, for different experiments, the η values should be monitored at identical time intervals of the chronopotentiometric pulse.

The electrode resistance, R', values derived from the chronopotentiometric experiments do not coincide with the electron-transfer resistances, R_{et}, obtained from the Faradaic impedance spectra, and the comparison of these values needs to be made with caution. While the electrode resistances, R', correspond to the entire current flux at the electrode, the electron-transfer resistances R_{et} correspond only to the Faradaic current at the electrode interface. Thus, in the chronopotentiometric experiment, the non-Faradaic current originating from the double-layer charging always affects the electrode resistance. At high concentrations of the redox probe ($>10^{-3}$ M), the double-layer charging current is negligible as compared to the Faradaic current. Under these conditions, it is expected that $R' \approx R_{et}$. Furthermore, the double-layer charging current increases with the potential applied onto the electrode. Thus, at high overpotential values, resulting at certain modifications of the electrode, deviations between the total electrode resistances derived from constant-current chronopotentiometry and the electron-transfer resistances determined by

Faradaic impedance spectroscopy may be observed, even at high concentrations of the redox probe. In contrast to the Faradaic impedance method, chronopotentiometry measurements are recorded within a few seconds.

Amplified Detection of Anti-DNP-Ab. The amplified detection of the anti-dinitrophenyl antibody, DNP-Ab (IgG from goat), using the biotin-labeled HRP-functionalized liposome was investigated according to Scheme 1. A dinitrophenyl-L-cysteine monolayer was assembled as a sensing interface on an Au electrode. In the presence of the DNP-Ab, the antigen−antibody complex is formed on the electrode. This process is amplified by the association of the biotinylated anti-goat IgG antibody (Fc-specific, from rabbit), followed by the binding of avidin and the biotinylated-HRP liposome probe. Subsequently, the HRP-functionalized liposome is used for the biocatalyzed oxidation of 4-chloronaphthol by H_2O_2 to yield the insoluble product **2** on the electrode.

Figure 1A shows the Faradaic impedance spectra (in the form of a Nyquist plot) upon the buildup of the assembly and the biocatalyzed precipitation of **2** on the electrode. The binding of the DNP-Ab and then the anti-antibody increases the interfacial electron-transfer resistances to $R_{et} = 1.36$ and 2.60 kΩ, respectively. The association of avidin and of the liposomes further increases the electron-transfer resistances at the electrode to $R_{et} = 3.47$ and 4.96 kΩ, respectively. The binding of the proteins (antibodies or avidin) to the interface generates a hydrophobic insulating layer on the electrode. This introduces a barrier for electron transfer to the redox label, $Fe(CN)_6^{3-}/Fe(CN)_6^{4-}$, in solution, resulting in an increase in the electron-transfer resistances at the electrode. The association of the negatively charged liposomes results in a micromembrane that electrostatically repels the redox probe. This electrostatic barrier is reflected by an increase in the interfacial electron-transfer resistance. Figure 1A, curve f, shows the impedance spectrum after the biocatalyzed precipitation of **2** on the electrode which proceeds for 10 min. The interfacial electron-transfer resistance increases to $R_{et} = 7.39$ kΩ. This is attributed to the insulation of the electrode support by the insoluble precipitate. The solid lines in the spectra shown in curves b−f correspond to the theoretical fits using an equivalent circuit that consists of the solution resistance, R_s, in series to a subcircuit that includes the electron-transfer resistor element in parallel to the double-layer capacitance. That is, the changes in the electron-transfer resistance and capacitance as a result of the binding of any of the proteins or the liposomes to the electrode surface can be modeled by an equivalent circuit that includes an electron-transfer resistor element, R_{et}, and a capacitor, C_i (see Scheme A, Supporting Information). The resistor element is always the sum of the resistances in the previous modification steps with the added resistance value, $\Delta R_{et}{}^i$, corresponding to the specific modification step. For example, the calculated resistance element upon the association of avidin is 1.4 kΩ and it corresponds to the sum of the calculated resistances as a result of the binding of the DNP-Ab, the anti-antibody, and the added resistance element as a result of the association of avidin, 4.3 kΩ. The capacitance values of each of the elements increase in magnitude upon the stepwise binding of the different components (decrease in the total capacitance of the system; $1/C_{total} = \Sigma 1/C_i$). Table 2 summarizes the different resistance and capacitance values calculated from the respective experimental impedance spectra
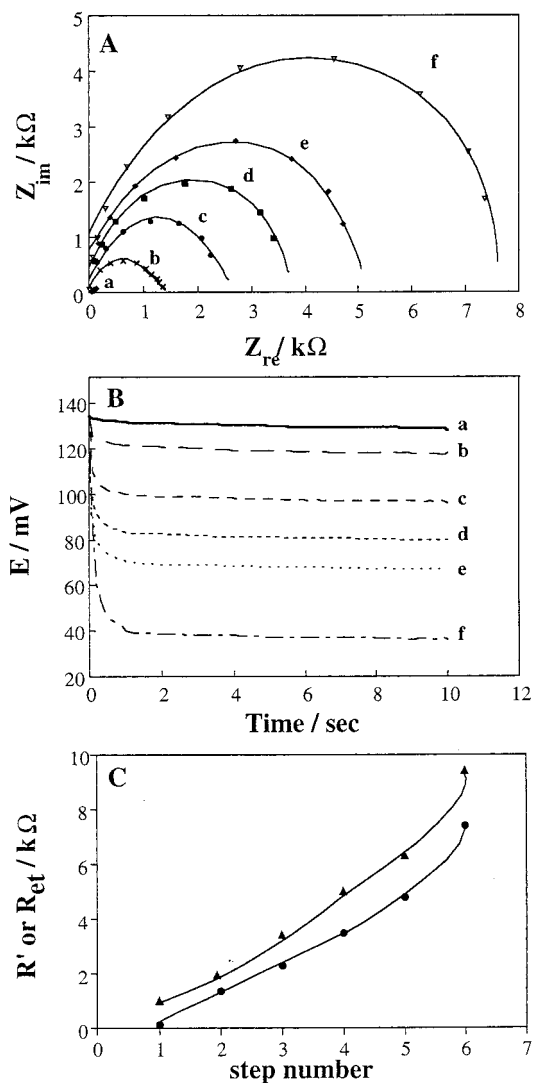

Figure 1. Sensing of the DNP-antibody with the DNP-antigen-modified electrode according to Scheme 1: (A) Nyquist plots (Z_{im} vs Z_{re}) for the Faradaic impedance measurements in the presence of 10 mM $[Fe(CN)_6]^{3-/4-}$ at (a) the DNP-antigen-modified electrode, (b) the DNP-antigen-modified electrode treated with 0.1 ng·mL^{-1} DNP-Ab, (c) after further addition of a biotinylated anti-anti-DNP-Ab (15 μg·mL^{-1}, 5 min), (d) the DNP/DNP-Ab/anti-antibody-biotin complex-modified electrode after reaction with avidin (100 ng·mL^{-1}, 15 min), (e) after addition of the biotin-labeled HRP-modified liposomes (1.46 × 10^{-11} M, 30 min), and (f) after allowing the biocatalyzed precipitation process to occur in the presence of **1**, 1 × 10^{-3} M and H_2O_2, 1.5 × 10^{-4} M, for 10 min. (B) Transient potential changes upon the application of a chronopotentiometric pulse (maintaining 10 μA for 10 s) in the presence of 10 mM $[Fe(CN)_6]^{3-/4-}$, curves a−f correspond to the systems described in (A). (C) Electron-transfer resistance, R_{et}, derived from the Faradaic impedance measurements (●); and electrode resistance, R', derived from the chronopotentiometric measurements (▲) resulting from the steps of modification of the electrode. Step 1, the DNP-modified electrode; step 2, the DNP-modified electrode after its interaction with the DNP-antibody (0.1 ng·mL^{-1}, 5 min); step 3, further interaction of the modified electrode with the anti-anti-DNP-biotin-labeled anti-antibody; step 4, further interaction with avidin; step 5, upon introduction of the electrode with the biotin labeled-HRP-modified liposome; step 6, after allowing the biocatalyzed precipitation process to occur for 10 min. All measurements were conducted in a phosphate buffer, pH 7.3, 0.1 M. Incubations were performed in a saline phosphate buffer, pH 7.3, 0.1 M.

Table 2. Calculated Values for the Electron-Transfer Resistance and Capacitance at the Electrode Surface upon the Amplified Sensing of the DNP-Ab

step no.[a]	R_i (Ω)	R_{total} (Ω)	C_i (μF)	C_{total} (μF)
1	1364	1364	5	5
2	1506	2870	13	3.6
3	1442	4312	60	3.45
4	1766	6078	130	3.33
5	2709	8787	27	2.97

[a] Steps 1−5 are depicted in Scheme 1.

Figure 2. (A) Nyquist plot (Z_{im} vs Z_{re}) for the Faradaic impedance measurements in the presence of 10 mM [Fe(CN)$_6$]$^{3-/4-}$ for the sensing of different concentrations of the DNP-antibody with the DNP-antigen-modified electrode and using the biotin-labeled anti-anti-DNP-antibody, avidin, and the biotin-labeled HRP-functionalized liposome, for the amplified sensing of the DNP-Ab according to Scheme 1. In all experiments the probe solution includes **1**, 1×10^{-3} M and H$_2$O$_2$, 1.5×10^{-4} M, and precipitation of **2** proceeds for 10 min. DNP-antibody concentrations: (a) 0.01, (b) 0.1, (c) 1, and (d) 10 ng·mL^{-1}. (B) Calibration plot corresponding to the interfacial electron-transfer resistances, R_{et}, as a function of the log of the analyte DNP-antibody concentrations. All measurements were conducted in a phosphate buffer solution, pH 7.3, 0.1 M.

using the equivalent electronic circuits shown in Scheme A, Supporting Information.

Figure 1B shows the $E-t$ chronopotentiometric transients upon the buildup of the layered assembly shown in Scheme 1 and upon the biocatalyzed precipitation of **2**. We realized that upon each step of formation of the layered assembly, the overpotential required to reduce the redox label in solution increases, as compared to the reduction of the redox probe by the bare electrode, curve a. For example, the formation of the complex between the antigen monolayer and the DNP-Ab results in an overpotential of $\Delta E = 13$ mV, curve c, whereas the association of the biotinylated-HRP-modified liposome to the interface, curve e, yields an overpotential of $\Delta E = 63$ mV. Also, the biocatalyzed precipitation of **2** on the electrode is accompanied by a substantial increase in the overpotential for the reduction of the redox-probe, curve f, $\Delta E = 94$ mV. The respective values of the overpotential for the reduction of the redox probe in the electrolyte solution can be translated to the corresponding values of the electrode resistance, eq 2. Figure 1C shows the plot of the electron-transfer resistances at the electrode interface, deduced from the impedance spectra, for the different steps of analysis of the DNP-Ab according to Scheme 1, and the respective electrode resistances of the electrode (R'), extracted from the corresponding chronopotentiometric experiments. The results indicate a reasonable correlation between the electrode resistances, R', and the interfacial electron-transfer resistances, R_{et}.

The amounts of biotinylated-antibody, avidin, and biotinylated-HRP-modified liposomes that are linked to the electrode are controlled by the amount of the analyte DNP-Ab that is associated with the surface. The content of the DNP-Ab on the surface is dominated by the bulk DNP-Ab concentration in the sample. The amount of the insoluble product **2** formed on the electrode, at a fixed precipitation time interval, is controlled by the HRP-functionalized liposomes associated with the electrode and, thus, directly related to the DNP concentration in the sample. Figure 2A shows the impedance spectra that correspond to the precipitation process of **2** upon the analysis of different concentrations of DNP-Ab. The electron-transfer resistances of the electrode increase as the bulk concentration of the analyte DNP-Ab is elevated, thus allowing the quantitative analysis of the antibody (Figure 2B). A very sensitive detection limit for the DNP-Ab that corresponds to 1×10^{-11} g·mL^{-1} is accomplished.

We find that the biotin-labeled HRP-functionalized liposomes not only function in the amplification of the analysis of the DNP-Ab but act as "cleaning agents" for nonspecific binding and thus enhance the sensitivity of the sensing process. In a control
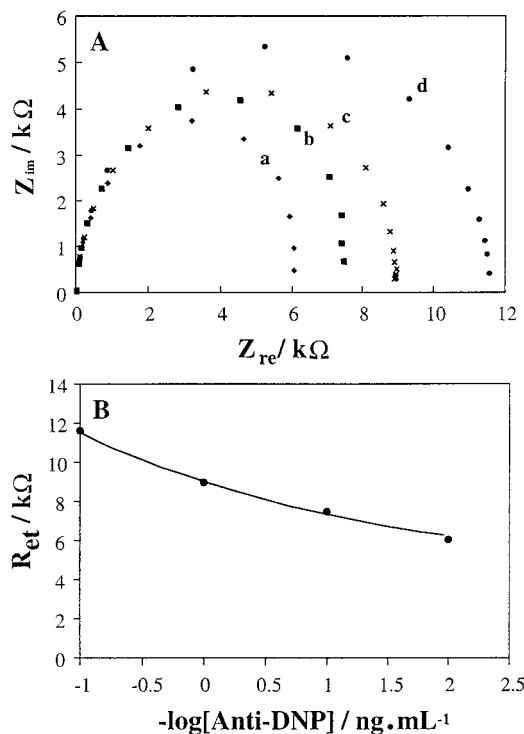
experiment, the antigen-functionalized interface was interacted with the foreign anti-glucose oxidase antibody from mouse and then treated with the biotinylated anti-goat antibody and avidin. Faradaic impedance measurements reveal that the electron-transfer resistance at the electrode increases from $R_{et} = 0.4$ kΩ to $R_{et} = \sim 1.8$ kΩ after this three-step treatment. This increase in the electron-transfer resistance is attributed to the nonspecific binding of the different proteins to the surface. Further treatment of the surface with the functionalized liposomes leads, after rinsing, to the original electron-transfer resistance, characteristic of the antigen-modified electrode, $R_{et} \cong 0.4$ kΩ. That is, treatment of the interface with the liposomes removes the nonspecifically bound proteins from the interface. Presumably, the association of these nonspecifically bound proteins, i.e., biotinylated anti-goat antibody and avidin, to the large liposomes facilitates their removal from the electrode. The resulting surface, after treatment with the liposomes, does not lead to any increase of the electron-transfer resistance upon an attempt to induce the biocatalyzed precipitation of **2**, implying that no liposomes are bound to the surface. The electrode surface retains its activity for the sensing of the DNP-Ab analysis, and the results shown in Figure 1A could be reproduced by the electrode that was used in the control experiment.

Finally, the electron-transfer resistance at the electrode, as a result of the accumulation of the insoluble product **2**, is controlled by the time allowed for the biocatalyzed precipitation. The DNP-Ab, at a constant concentration of 1×10^{-10} g·mL^{-1}, was analyzed according to Scheme 1 by allowing the biocatalyzed precipitation of **2** to proceed for different time intervals. The electron-transfer resistance increases as the biocatalyzed precipitation is prolonged (see Supporting Information). For example, the electron-transfer resistance increases from $R_{et} = 3.2$ kΩ after 8 min of precipitation to $R_{et} = 8.0$ kΩ after 15 min of precipitation. Thus, the sensitivity of the sensing of the antibody may be improved by prolonging the time interval for the precipitation of the insoluble product on the electrode surface.

Amplified Sensing of DNA. The biotin-labeled HRP-functionalized liposomes were also employed as probes to amplify the sensing of DNA, according to Scheme 2. Specifically, a sensing electrode for the oligonucleotide **3**, which is a model assembly for the Tay-Sachs genetic disorder mutant, was developed. The TS disease[34] is caused by hexoseaminidase deficiency, the enzyme that degrades GM$_2$ ganglioside to GM$_3$. It appears at ~6 months of age and is fatal usually in early childhood. Affected children become blind and physically and mentally regressed. The disease originates from a genetic disorder that is frequent in Jews of Eastern European descent. In a recent survey,[35] it was reported that 1 in 30 Jews of Eastern European descent in the United States and Canada is a carrier of the defective gene.

The 18-base oligonucleotide **4** includes 12-bases that are complementary to the target analyte DNA **3**, and acts as the probe for the recognition of the analyte, a 5-base thymine thiophosphate tag (Ts), for the immobilization on an Au surface, and a single T-base that links the primer to the tag. The oligonucleotide **4** was immobilized on an Au electrode. Its surface coverage corresponds to 1.4×10^{-11} mol·cm^{-2}. The surface coverage was determined according to Tarlov's method.[36] Figure 3 shows the Faradaic impedance spectra upon the analysis of the analyte DNA **3** according to Scheme 2 and using the biotinylated-HRP liposomes as probe for the amplified detection of **3**. The association of the analyte **3** to the sensing interface to form the ds assembly is accompanied by an increase of the electron-transfer resistance at the electrode from 0.2 to 0.39 kΩ. Further association of the biotinylated oligonucleotide **5** increases the interfacial electron-transfer resistance to 0.79 kΩ, curve d. These results are consistent with the fact that the sequential formation of the three-component ds assembly on the surface electrostatically repels the redox label, Fe(CN)$_6^{3-}$/Fe(CN)$_6^{4-}$, and thus the interfacial electron-transfer resistance gradually increases upon the buildup of the assembly. The association of avidin, curve e, further increases the interfacial electron-transfer resistance, as a result of the partial hydrophobic insulation of the electrode support. The association of the biotin-functionalized HRP liposome substantially increases the electrode transfer resistance, curve f, $R_{et} = 1.5$ kΩ. The

(34) Gravel, R. A.; Clarke, J. T. R.; Kaback, M. M.; Mahuran, D. J.; Sandhoff, K.; Suzuki, K. In *the Metabolic and Molecular Basis of Inherited Disease*; Scriver, C. R., Beaude, A. L., Sly, W. S., Valle, D., Eds.; McGraw-Hill: New York, 1995; Vol. 2, pp 2839−2879.

(35) Kaback, M.; Lim-Steele, J.; Dabholkar, D.; Brown, D.; Levy, N.; Zeiger, K. *J. Am. Med. Assoc.* **1993**, *270*, 2307−2315.

(36) Steele, A. B.; Herneand, T. M.; Tarlov, M. *J. Anal. Chem.* **1998**, *70*, 4670−4677.
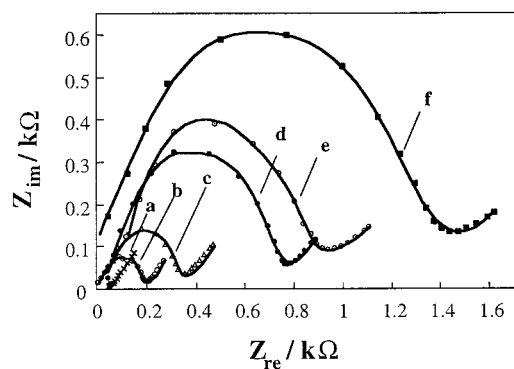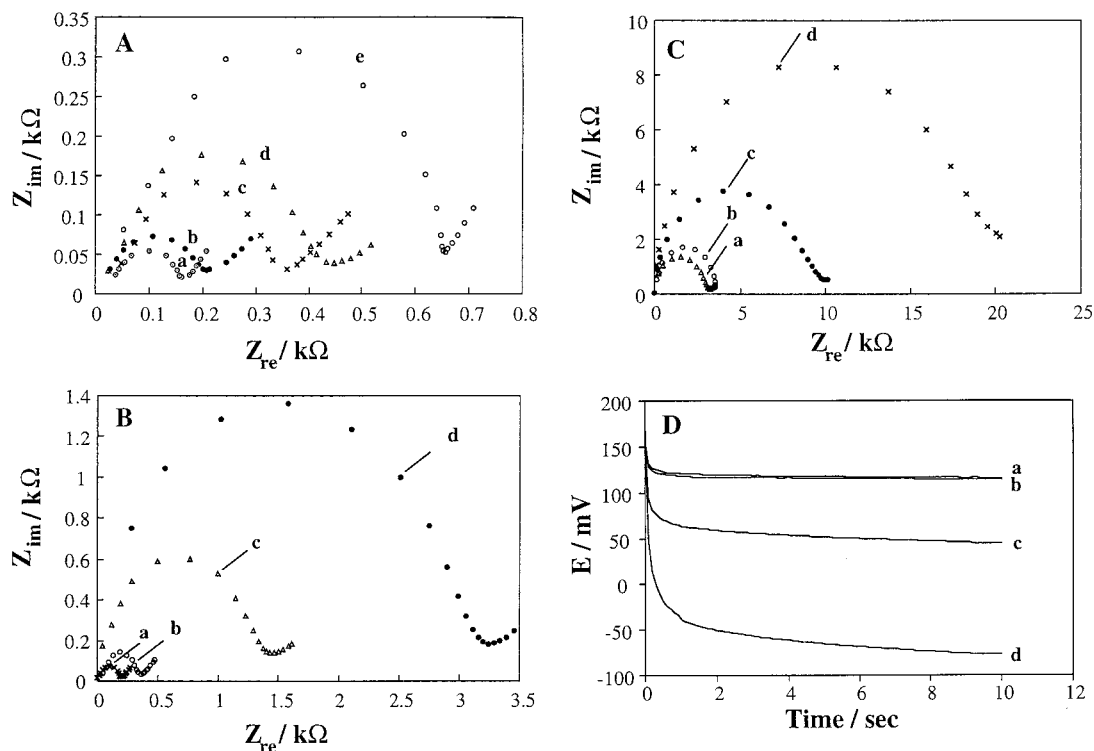
Figure 3. Faradaic impedance spectra (in the form of Nyquist plots, Z_{im} vs Z_{re}) that correspond to (a) a bare Au electrode; (b) the **4**-functionalized electrode; (c) after interaction of the sensing electrode with **3**, 6.5×10^{-12} M, 1 h; (d) after treatment of the resulting electrode with **5**, 7×10^{-8} M, 1 h; (e) after interaction with avidin (200 ng·mL,$^{1-1}$ 20 min); and (f) after interaction of the interface with the biotin-HRP-labeled liposomes (1.46×10^{-11} M, 30 min). Hybridization was conducted in a 2 × SSC buffer. In all measurements Fe(CN)$_6^{3-/4-}$, 1×10^{-2} M is used as redox label.

increase of the electron-transfer resistance upon binding of the negatively charged liposomes is attributed to the electrostatic repulsion of the redox label, Fe(CN)$_6^{3-}$/Fe(CN)$_6^{4-}$, by the liposomes that act as a micromembrane. The solid lines in the impedance spectra shown in Figure 3 correspond to the theoretical fit of the experimental data according to an equivalent circuit that includes the solution resistance in series to a subcircuit consisting of the interfacial electron-transfer resistance in parallel with the double-layer capacitance (see Scheme A, Supporting Information). The buildup of the double-stranded assembly with the linked liposomes was also examined by chronopotentiometry. The electrode resistances deduced by the latter method are very similar to the interfacial electron-transfer resistances, determined by Faradaic impedance spectroscopy (see Supporting Information).

Figure 4A shows the Faradaic impedance spectra upon the treatment of the sensing interface with different concentrations of the analyte DNA. As the bulk concentration of **3** increases, the interfacial electron-transfer resistance increases, implying that a higher content of the analyte is linked to the interface. One may realize that the association of the analyte **3** is still detectable at a bulk concentration of 6.5×10^{-13} M. Each of these sensing interfaces was subjected to the two-step amplification path that involves the binding of the liposomes to the interface and the secondary biocatalyzed precipitation of **2** on the electrodes by the HRP-functionalized liposomes. Figure 4B exemplifies the two-step amplification process for the sensing of the low concentration of DNA, 6.5×10^{-13} M. It can be seen that while the association of the analyte results in a minute increase in the electron-transfer resistance, $\Delta R_{et} = 0.18$ kΩ, the binding of the liposome increases the electron-transfer resistance by 1.1 kΩ, curve c, and the biocatalyzed precipitation of **2** for 10 min further increases the electron-transfer resistance by 2.0 kΩ. Figure 4C shows the Faradaic impedance spectra resulting upon the precipitation of the insoluble product on the electrode surfaces that sense different concentrations of the analyte DNA **3**. As the bulk concentration of DNA increases, the amount of precipitate is higher, as reflected by the elevated electron-transfer resistance at the electrode. This

Figure 4. (A) Faradaic impedance spectra (Nyquist plots, Z_{im} vs Z_{re}) measured for the **4**-functionalized electrode. (a) The **4**-modified electrode prior to hybridization; (b–e) after interaction of the sensing interface with the analyte **3** at concentrations corresponding to 6.5×10^{-13}, 6.5×10^{-12}, 6.5×10^{-11}, and 6.5×10^{-10} M, respectively. The hybridizations were performed in $2 \times$ SSC buffer. (B) The two-step amplified sensing process of the DNA **3** by the biotin-HRP-modified liposomes and the biocatalyzed precipitation of **2** on the electrode support: (a) after modification of the electrode with the sensing interface **4**; (b) upon interaction of the sensing interface with the analyte **3**, 6.5×10^{-13} M; (c) amplification of the signal after addition of the complementary biotin-labeled oligonucleotide **5**, avidin, and further interaction of the assembly with the biotin-HRP-labeled liposomes; (d) a second amplification stimulated by the biocatalyzed precipitation of **2** in the presence of 1×10^{-3} M **1** and 1.5×10^{-4} M H_2O_2 for 10 min. (C) Sensing of different concentrations of the analyte **3** by the two-step amplification (cf. Scheme 2), where the **4**-modified electrode was subjected to different concentrations of **3** followed by the interaction of the interface with **5** and then with avidin and further with the biotin-HRP-labeled liposomes. The spectra correspond to the electrodes after the biocatalyzed precipitation of **2** is stimulated for 10 min in the presence of 1.5×10^{-4} M H_2O_2 and 1×10^{-3} M **1**. Analyte concentrations: (a) 6.5×10^{-13}, (b) 6.5×10^{-12}, (c) 6.5×10^{-11}, and (d) 6.5×10^{-10} M. (D) Transient potential changes upon the application of a chronopotentiometric pulse (maintaining 10 μA for 10 s) in the presence of 10 mM $[Fe(CN)_6]^{3-/4-}$ to the electrodes modified according to (C).

is consistent with the fact that at high bulk concentrations of DNA the amount of the liposome-probe associated with the interface increases, resulting in enhanced precipitation of **2**. Constant-current chronopotentiometry experiments yield similar conclusions. Figure 4D shows the $E{-}t$ transients resulting upon the biocatalyzed precipitation of **2** on the electrodes that sense different concentrations of the analyte DNA **3** (analogous system shown in Figure 4C). The overpotentials for the reduction of the redox label, $Fe(CN)_6^{3-}/Fe(CN)_6^{4-}$, increase as the bulk concentration of DNA is higher, implying that the insulation of the electrode by the insoluble precipitate is enhanced. The electrode resistances extracted from the overpotential values, eq 2, are very similar to the respective electron-transfer resistances deduced from the Faradaic impedance spectra.

The sensitivity for the sensing of the DNA can be controlled by the time interval employed for the biocatalyzed precipitation of **2** by the HRP-functionalized liposome. The analyte DNA **3** was sensed at a constant concentration that corresponds to 6.5×10^{-12} M, according to Scheme 2, using variable time intervals for the precipitation of the insoluble product **2**. The interfacial electron-transfer resistances at the electrode were characterized by Faradaic impedance spectroscopy and constant-current chrono-potentiometry (see experimental details in the Supporting Infor-

mation). The layered assembly on the electrode, which senses **3** and includes the biocatalytic liposome, exhibits an electron-transfer resistance of ~ 2 kΩ. After the biocatalyzed precipitation of **2**, the electron-transfer resistance at the electrode surface increases to $R_{et} = \sim 150$ kΩ. The increase of the electron-transfer resistance at the electrode support is nonlinear, and while after 5 and 10 min of precipitation, the $_{et}$ values increase by 7 and 23 kΩ, respectively, after 20 min of precipitation of **2**, the R_{et} value is 150 kΩ. This electron-transfer resistance represents a saturation value. Presumably, the insoluble precipitate covers the biocatalytic sites and this blocks further accumulation of the insoluble product. The nonlinear increase in the electron-transfer resistance at the electrode probably originates from the fact that the insoluble product on the electrode acts as a nucleation site for the subsequent precipitation of **2**. This facilitates the unidimensional growth of the product over the two-dimensional coverage of the electrode surface. Again, the formation of the insoluble product on the electrode at time intervals of precipitation can be followed by chronopotentiometry (see Supporting Information). As the insoluble product accumulates on the electrode, the overpotential for the reduction of the redox probe increases, indicating that the electrode resistance is higher.
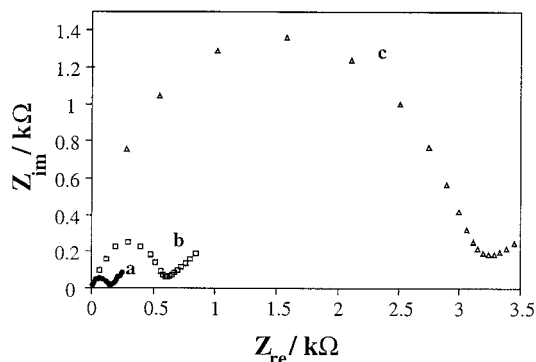
Figure 5. Faradaic impedance spectra (Nyquist plots, Z_{im} vs Z_{re}) corresponding to (a) the **4**-functionalized sensing electrode; (b) after pursuing the full procedure as described in Scheme 2, using the normal gene **3a** as the analyte (1.3×10^{-8} M), addition of the biotin labeled oligonucleotide **5**, avidin, and biotin-HRP-labeled liposome and conduction of the biocatalyzed precipitation of **2** for 10 min; (c) after treatment of the electrode generated in step b with the mutant **3**, 6.5×10^{-12} M, biotin-labeled oligonucleotide **5**, avidin, and then biotin-HRP-labeled liposome and conduction of the biocatalyzed precipitation of **2**. The precipitation was conducted for 10 min in the presence of **1**, 1×10^{-3} M, and H_2O_2 1.5×10^{-4} M.

The specificity of the DNA sensor is a major issue that needs to be addressed. In a control experiment, the **4**-functionalized electrode was treated with a *high* concentration, 1.3×10^{-8} M, of the normal gene **3a** and further treated with the biotinylated oligonucleotide **5** and avidin, according to Scheme 2. These steps induce a minute change in the electron-transfer resistance of ∼0.1 kΩ, due to the negligible nonspecific adsorption of the components on the electrode. Treatment of the electrode with the biotinylated HRP-functionalized liposomes reveals, after rinsing, the nonspecific "cleaning effect", and the electron-transfer resistance at the electrode regenerates the original value characteristic to the **4**-functionalized electrode. This effect is attributed to the association of avidin and the biotin-labeled oligonucleotide **5** with the heavy liposomes that wash off the adsorbates. An attempt to stimulate the biocatalyzed precipitation of **2** on the electrode that was treated with the normal gene **3a**, 1.3×10^{-8} M, yielded the impedance spectrum shown in Figure 5, curve b. A semicircle with a very low interfacial electron-transfer resistance is observed, $R_{et} \cong 0.6$ kΩ. Treatment of this electrode with the mutant **3**, at a concentration of 6.5×10^{-12} M, results in, after precipitation, an interfacial electron-transfer resistance of $R_{et} = 3.4$ kΩ, Figure 5, curve c. Note that, with the target analyte **3** at a 2000-fold lower concentration than the normal gene, a 7-fold higher electron-transfer resistance is observed. Also, treatment of the **4**-functionalized electrode with denaturated calf thymus DNA did not yield any increase in the electron-transfer resistance at the electrode interface. Thus, the sensing of the Tay-Sachs mutant is very specific with the functionalized sensing electrode, and the normal gene is easily discerned from the analyte DNA.

Previous studies have employed peptide nucleic acids (PNA),[37] as primers, or applied of temperature-controlled duplex formation of mismatched double-stranded DNA,[38] in order to induce specific-

ity in the sensing processes. However, these approaches suffer from the fact that there is always an affinity between the mismatched nucleic acid and the primer PNA or oligonucleotide, thus enabling discernment of the target DNA from the mutant only at identical concentrations. In the present study, we highlight the differentiation between the analyte **3** and the normal gene **3a** at a concentration ratio of 1:2000. This originates from the careful design of the probe structure. The probe **4** is selected to include 12 bases complementary to the analyte **3**. This number of bases consists of the minimal sequence to generate a full double-stranded turn. The complementarity provided by the primer to the normal gene **3a** is insufficient to yield the double-stranded turn that lacks the thermodynamic duplex stability. This leads to the unprecedented specific sensing of **3**.

CONCLUSIONS

The present study employed biotinylated-HRP-functionalized liposomes as probes for the two-step amplification of antigen–antibody interactions and the detection of DNA. We demonstrate that the primary binding of the liposome to the interface generates a micromembrane environment that alters substantially the interfacial properties of the electrode. The secondary HRP-mediated precipitation of the insoluble product amplifies further the primary detection of the respective antibody or target DNA by the insulation of the electrode. We find that the insulation of the electrode by the precipitate is controlled by the analyte concentration in the sample (antibody or DNA), as well as by the time interval used for the precipitation process.

The electrochemical transduction methods, i.e., Faradaic impedance spectroscopy and chronopotentiometry, are used to follow the detection of the antibody or target DNA by the functionalized liposomes and the secondary biocatalyzed precipitation of **2**. While impedance spectroscopy is a very useful method to characterize fundamental interfacial properties of the electrode and its modification (electron-transfer resistance, capacitance), it has limited practical use in biosensor technology due to the long time required to accumulate a spectrum in a full-frequency range. Chronopotentiometry is a rapid detection method (a few seconds) and can easily be applied to follow the modification events on the surface.

Finally, an important conclusion of the present study relates to the specificity of the resulting immunosensor and DNA sensor electrodes. We find that the functionalized liposomes act as "cleaning agents" of nonspecific protein (antibody or avidin) or DNA adsorbates. The removal of the nonspecific adsorbates enables the selective sensing of the target analytes. This property of the functionalized liposomes is of importance in the very sensitive and specific detection of the Tay-Sachs DNA mutant.

SUPPORTING INFORMATION AVAILABLE

The Faradaic impedance spectra and constant-current chronopotentiometric transients corresponding to the analysis of the DNP-Ab or the target DNA **3** by the precipitation of the insoluble product **2** for different time intervals; the constant-current chro-

(37) (a) Wang, J. *Biosens. Bioelectron.* **1998**, *13*, 757–762. (b) Wang, J.; Palecek, E.; Nielsen, P. E.; Rivas, G.; Cai, X. H.; Shiraishi, H.; Dontha, N.; Luo, D.; Farias, P. A. M. *J. Am. Chem. Soc.* **1996**, *118*, 7667–7670.

(38) Caruana, D. J.; Heller, A. *J. Am. Chem. Soc.* **1999**, *121*, 769–774.

nopotentiometric transients corresponding to the stepwise assembly of the sensing interface for the DNA **3**; the interfacial electron-transfer resistances and the electron-transfer resistance of the electrode upon construction of the sensing interface for **3**, and the detection procedure of **3**, graphically presented; and a scheme that presents the equivalent circuit that corresponds to the buildup of the sensing interface and detection procedure for the DNP-Ab or the DNA **3**. This material is available free of charge via the Internet at http://pubs.acs.org.